Are there other tectonics than tidal despinning, global contraction and Caloris related events on Mercury? A review of questions and problems

Pierre G. Thomas

Laboratoire des Sciences de la Terre (UMR 5570), Ecole Normale Supérieure de Lyon, 46 allée d'Italie, 69364 Lyon cedex 07, France

Abstract. Mercury's tectonic activity was confined to its early history. A synthesis of classical references indicates that its tectonic activity was principally related to (1) a small change in the shape of its lithosphere by tidal despinning, (2) a small change in radius and area by shrinkage due to secular cooling, and (3) the Caloris related events. These activities produced the ancient tectonic grid, the lobate scarps, and the Calorian ridges, scarps and grabens, respectively. This low degree of activity was ultimately due to Mercury's small size. In spite of this apparent simplicity, some features are still intriguing. Detailed compilation of lineaments on the entire planet indicates that the grid is not similar to the theoretical despinning grid. Some trends are explained by despinning, but only with unusual mechanical properties of the Mercurian lithosphere, while some other trends are not explained at all by despinning. Examples of unexplained tectonic features in the same region are presented in this paper. Some circular depressions may be interpreted as the result of tectonic or volcano-tectonic subsidence (caldera?). Some exibit narrow and particularly straight grooves which cannot be explained as impact related features, and may be interpreted as open tectonic cracks. The Tolstoj area exhibits hills and grooves which cannot be interpreted as Tolstoj impact related features. Morphological and chronological studies indicate that these features would consist of the extensional tectonic features (horsts and grabens) developed on the convex top of a tectonically uplifted bulge. The tectonic development of this area occurred over a long period of time, and is probably due to a deep and long-lived internal source. These examples show the existence of large- and small-scale internal activities which affect Mercury's surface independently from global or impact related tectonics. Such activities must be taken into account in further models of Mercurian internal structure and history, and must be searched in data of future missions. A new Mercurian mission with a complete coverage of image

and altimetric/gravimetric data is thus necessary to understand the geology and the tectonic of Mercury. © 1997 Published by Elsevier Science Ltd. All rights reserved

Introduction

Mercury's tectonic activity was confined to its early history as a planet. A synthesis of classical references indicates that its tectonic activity was principally related to three kinds of phenomena. (1) Mercury's most ancient tectonic features consist of a fabric of fractures or weak zones that were impressed on the lithosphere before any presently recognizable topographic features were formed. This Mercurian grid was recognized by Fielder (1974) and Dzurizin (1978) and was commonly attribued to stresses that developed in Mercury's lithosphere due to tidal despinning. (2) The surface of Mercury is affected by numerous lobate and arcuate scarps, firstly studied by Murray *et al.* (1975), Strom *et al.* (1975), and Dzurizin (1978). The scarps are interpreted as thrusts and reverse faults supposed to be the result of a small change in Mercury's surface by shrinkage due to secular cooling, and global contraction, equivalent to 1–2 km decrease in the planet's radius. (3) The Caloris related events, which produced rings tectonics, the interior and exterior smooth plains tectonics, and the hilly and lineated terrains near the antipode of Caloris by focusing the seismic waves from the Caloris impact (Strom *et al.*, 1975; Schultz and Gault, 1975; McKinnon, 1981; Dzurizin, 1978). Fleitout and Thomas (1982) proposed also an interaction between the Caloris events and the Global contraction.

The volcanic history of Mercury was also confined to its early history (Trask and Guest, 1975; Spudis and Guest, 1988). The intercrater plains consist of old terrains, heavily cratered during the end of the post-accretional heavy bombardment. These old plains are locally embayed by younger units, which are probably lava flows. Some vol-

canic areas exhibit ridges which may be interpreted as dike-like volcanic extrusion (Dzurizin, 1978). The volcanic activity ended with the Smooth plains flooding which followed the Caloris impact.

This low degree of activity was ultimately due to Mercury's small size.

But, in spite of this apparent simplicity, many faint but real morphological features cannot be explained by the previously mentioned geological processes.

Is the global lineament pattern only due to tidal despinning?

Since the work of Fielder (1963) and Strom (1964), the word "lineament" is commonly used for all rectilinear features of unclear origin on planetary surfaces including valleys, ridges, scarps, rills, non-impact-related craters chains, linear portions of central peaks or crater rims, albedo contrasts and other linear alignments of unknown origin. On the Moon, the lineaments are not randomly oriented. Fielder (1963) and Strom (1964) both have shown that by deleting radial lineament systems associated with the major lunar impact basins, three prominent systems remain, trending approximately NW–SE, NE–SW and N–S. This result is interpreted in terms of tectonic stresses, producing a planetary-wide fault system termed the lunar grid. The origin of the grid is commonly attributed to stresses that developed in the Moon's lithosphere due to tidal spindown, first analysed by Burns (1976) and Melosh (1977). It is generally accepted that the Moon's 27 day resonant rotation period is the residual of an initially much faster rotation rate slowed by terrestrial tides. As the Moon despun, the equatorial bulge relaxed, the planet changed shape and the equator became shorter. Melosh (1977) examined the tectonic consequences of despinning and equatorial shortening: a zone of N 60°E and N 120°E trending strike-slip faults forms in intermediate latitudes, a zone of E–W trending normal fault in polar latitudes, and an equatorial zone of N–S trending thrust faults if the lithosphere is thinner than 0.05 of the planet's radius (Fig. 1). Despinning associated with a global contraction or expansion will induce alterations in the relative intensity and in the latitudinal distribution of lineaments, but will not change their directions (Pechmann and Melosh, 1979). The grid pattern was created very early in the Moon's history, but late local stresses, due to impacts or other causes could reactivate faults along these pre-existing directions, resulting in the valley, ridges, and other features observed today.

Several authors (see, e.g. Fielder, 1974; Trask and Guest, 1975; Masson and Thomas, 1977; Dzurizin, 1978; Thomas, 1978; O'Donnell, 1980; Schaber and McCauley, 1980) have described local or global Mercurian lineament patterns, and found N50°, N130°, and a weaker set of N–S trending lineaments. It is generally accepted that Mercury's present 59 day resonant rotation period is the residual of an initially faster rotation rate slowed by solar tides. The origin of the Mercurian grid is thus commonly attributed to despinning, because of the similarity of the Lunar and Mercurian grids trending. Nevertheless, this Mercurian grid was proposed without an exhaustive and
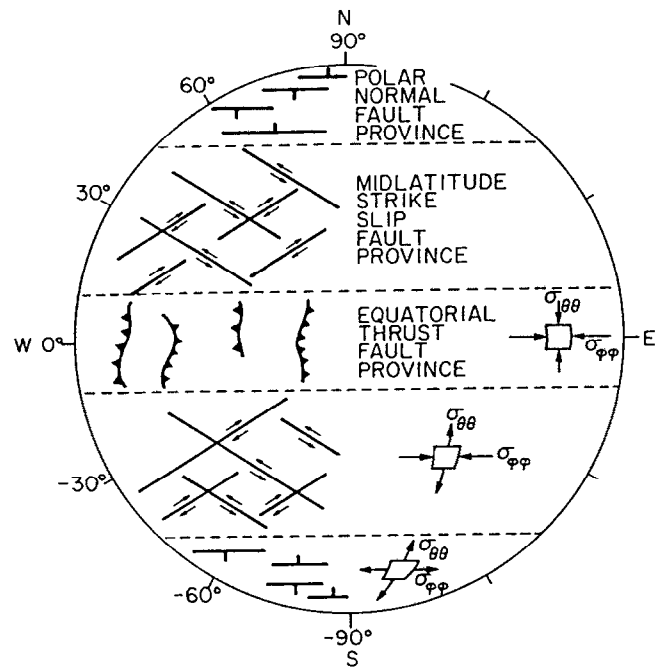

Fig. 1. Tectonic of a despun planet (figure after Melosh (1977))

detailed compilation of lineaments. In order to further characterize the tectonic grid patterns proposed earlier, such a compilation of lineaments was undertaken (Thomas and Masson, 1983). Two thousand five hundred high- and medium-resolution pictures of Mercury were analysed looking for all rectilinear or broadly arcuate features. All these features were mapped, except those which were obviously not due to tectonic effect, such as secondary crater chains. This resulted in lineament maps for the nine known quadrangles of Mercury. Fourier transforms of the mapped lineaments were generated for each quarter of a quadrangle map of Mercury, producing an azimuthal rose diagram showing the relative importance of the lineament directions. The resulting Mercurian grid is illustrated by plotting the obtained Fourier transforms on a map of Mercury (Fig. 2).

In order to determine the origin of these lineaments, we assumed that the lineaments resulting from radial cracks associated with an impact are oriented in all azimuths. However, tectonic lineaments are not randomly oriented in azimuth: reverse faults are trending perpendicularly to the main horizontal stress, normal faults are trending parallelly to this stress and the strike-slip faults are theoretically oriented 30–35° with respect to this main horizontal stress. Consequently, it is assumed that major trends in the azimuthal distribution of lineaments may indicate the influence of tectonic processes. A planetary-wide homogeneity of this distribution would probably indicate the existence of a grid pattern.

On the basis of this map, the following conclusions may be drawn:

1. The lineaments are not randomly oriented for each quarter of the quadrangle, but exhibit well-defined trends (Fig. 2).
2. The lineament trends show a gap in the azimuthal direction of solar illumination, suggesting that the illumination angle greatly influences the detectability
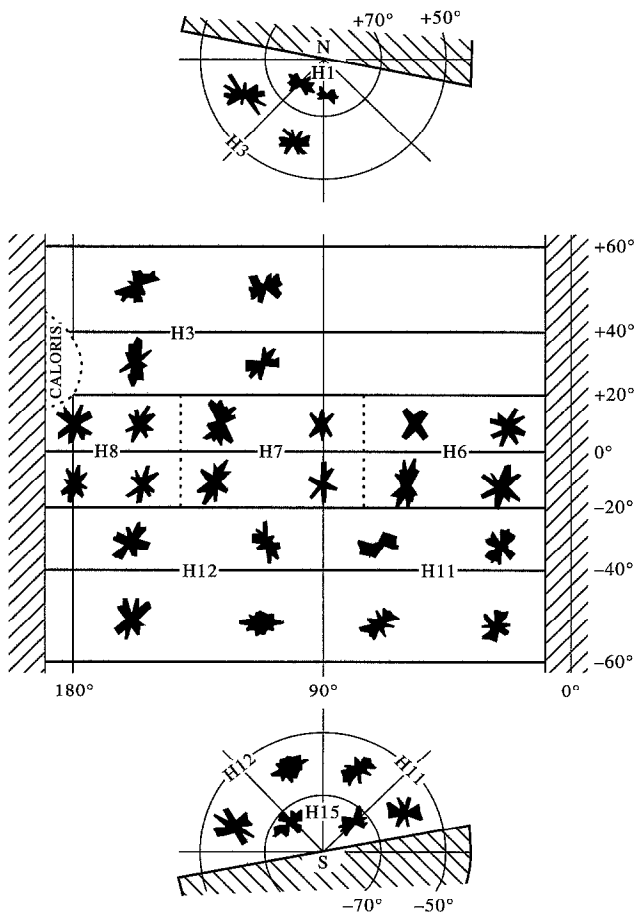
Fig. 2. Global disposition of lineaments on Mercury. Each rose diagram is a Fourier transform of all mapped lineaments in each quarter of a quadrangle. This map clearly exhibits that different maxima are not randomly oriented, especially in the equatorial areas, where four trends are well represented (N20°, N50°, N135° and N160°) (figure from Thomas and Masson (1983))

of lineaments. This effect, which emphasizes lineaments oriented perpendicularly to the sunlight direction and minimizes the parallel ones, would produce a unimodal distribution, different from the multiple maxima really observed. The combination of these two results indicates the existence of one or more tectonic processes which are locally responsible for the lineament directions.

3. The global map (Fig. 2) shows that the different maxima are not randomly oriented, but are more or less constant in azimuth for the entire planet, especially in the low-latitude areas (between +60° and −60° latitude), where four directions are well represented: N20° (the most significant), N50°, N135° and N160° (the least significant). In the polar areas, the different maxima and the azimuthal distribution of these maxima are not as well defined although an E–W direction is common.

Thus, most of the lineaments seem to correspond to a pre-existing grid pattern. The abundance of lineaments is higher in the intercrater plains than in the smooth plains, indicating the great age of the majority of the lineaments. On all the terrestrial planets, large impact craters can cause tectonic stresses beyond their rims, which generally

reactivate the local pre-existing tectonic trends (Strom, 1964; Eppler et al., 1983). Features of this origin may exist around the Caloris basin (Thomas and Masson, 1984). Moreover, the impact which produced the Caloris basin also caused tectonic movements at its antipodal point (Schultz and Gault, 1975). These movements around and antipodal to the basin both show the same orientation as those in the intercrater plains. Thus, the lineament grid seems to have existed before the end of the major bombardment, and certainly before the Caloris impact.

Theoretically, despinning induces N60°, N120° and N–S trending lineaments in the low latitudes, with also an E–W trend in the polar areas (Burns, 1976; Melosh, 1977). The despinning model was proposed by previous authors to explain the local N50° and N130° trending lineaments. But our work concerns the entire known planet, and not only local areas. The difference between the observed and the theoretical grids (N50° and N135° versus N60° and N120°) seems too important to be neglected. The angle 2α of two conjugated strike-slip faults is theoreticaly 60° in natural stony material; this angle 2α is 85° on Mercury. Two solutions may be considered. (1) The Mercurian lithosphere is not made by brittle stony material, but rather by low cohesive or relatively ductile material with a 2α angle $\ll 60°$. (2) The N50° and N135° trending lineaments are not conjugated strike-slip faults due to an E–W main horizontal stress, i.e. the N50° and N135° lineaments are not due to tidal despinning. Moreover, the despinning model fails to explain the lack of a N–S lineament trend and the presence of the important N20°E and the weak N160°E lineament trends.

Other origins of grids were proposed (Melosh, 1980a,b; Helfenstein and Parmentier, 1985). They calculated the theoretical stress fields and the related grids generated by reorientation, orbital recession or orbital excentricity change. A possible reason why the Caloris basin lies on the axis of the minimum moment of inertia is that a large positive free-air anomaly, or mascon, is associated with Caloris (Murray and the Mariner 10 Imaging Team, 1974). Thus, it is possible that this basin altered the orientation of the planetary surface with respect to the rotational pole, and even its orbital parameters. Such disturbances theoretically could induce a global lineament grid pattern. The Mercurian grid, which already existed before the Caloris impact, exhibits lineament trends different from those predicted by Melosh or Helfenstein and Parmentier's theories. It is unlikely that the grid is due to such a disturbance. Moreover, the present orientation of the grid is almost symmetrical with regard to the actual equator, and could not be the result of the reorientation of a pre-existing pattern.

No single model explains the observed grid completely. The tidal despinning partially explains this grid if the Mercurian lithosphere material is made of an unusual material with an important 2α angle, but cannot be the only mechanism that changed the planet's shape. This could reflect deficiencies in the analytical forms of this model, or unmodelled properties of the Mercurian lithosphere. Further theoretical studies, comparison between other planetary lineament grids, and mainly the study of the unknown side of Mercury are required to provide significant understanding of this intriguing Mercurian grid.

Local tectonic activities

Mercury is not considered as a tectonically active planet. Discussions of the tectonic features of Mercury generally describe only the lobate scarps, the Caloris related events, and the lineaments pattern. Nevertheless, some local areas exhibit morphological features which may be due to tectonic motions of internal origin, but which do not seem to be related to a global model. In order to characterize such areas, we describe here as examples three regions in the southern part of the Tolstoj quadrangle (H8), which show three different scales of tectonic motions. These examples are chosen in the H8 quadrangle, because of its relatively high resolution images, good sunlight conditions and partial stereoscopic coverage.

The Kalidasa–Milton area (Fig. 3)

This area exhibits two troughs which cannot be explained as coalescent secondary impact crater chains.

The first trough joins two subdued unnamed craters ($-13°$ lat., $183°$ long. to $-16°$ lat., $184°$ long., U_1 and U_2 on Fig. 3). It is a N20° trending trough, parallel to the main trend of the Mercurian grid. This trough is absolutely rectilinear, it cuts the two craters' rims, its morphology is sharper and younger than the two cut craters, and also cuts the Smooth Plain which embayed the northern crater.

The second trough lies 150 km to the south-east of the first one, with cutting Kalidasa's rim (K on Fig. 3). It is a N160° trending trough, parallel to one trend of the grid. It begins with cutting Kalidasa's rim. Its width is approximately 500–1000 m, its length is about 250 km. It is remarkably rectilinear, even crossing topographic features. It widens crossing the Milton rim (M on Fig. 3), and transforms as a broad depression inside the smooth plain which fills the Milton crater.

Such troughs are morphologicaly different from secondary crater chains which exist for example in the northern surroundings of Kalidasa. The origin of such troughs is impossible to determine with the low resolution Mariner 10 images. Dzurizin (1978) described ridges which are interpreted as dike-like volcanic extrusions that followed a pre-existing fracture of the Mercurian grid. These ridges are about the same size as the Kalidasa–Milton troughs. It is possible to provisionally propose that these rectilinear troughs are non-magmatic open cracks.

The Phidias area (Fig. 4)

The crater Phidias ($+11°$ lat., $150°$ long.) has unusual characteristics. It is filled by smooth plains material, and classified as a very old C_2 crater by Schaber and McCauley (1980). Despite the absence of secondaries, central peak and wall terraces, it exhibits a very sharp break between wall and floor materials, and walls and surrounding plains. This wall is sharp in the northern part of its rim where it is circular in plan. It is also sharp on the eastern rim, where it is rectilinear in plan with a N20° trend. In the western part, the wall consists of en echelon rectilinear segments trending N20°. The SSE part of the rim is subdued, and the floor–wall boundary is indistinct. The SSW part of the rim is crosscut by a very old "ghost" crater (older than C_1 according to Schaber and McCauley (1980)).

Outside the Phidias crater, the terrains between Tyagaraja and Phidias seem to be affected by relatively subdued horst and graben.

It is difficult to envisage how impact-related phenomena could be the only origin of many of the characteristics described above, especially with regard to the apparent differences in ages for the Phidias walls, and the geometric relationship between Phidias and the ghost crater: it is impossible for the rims of one single crater to be different in age, and that an old impact crater cuts a younger one. We thus propose that the Phidias depression is not due to an impact, but rather due to a tectonic (or volcano-tectonic) subsidence of a nearly circular area. The subsidence resulted in fault walls around three-quarters of the depression, controlled by the N20°E trend, the most important direction of the Mercurian grid. This subsidence may be described as a caldera-like motion.

The Tolstoj–Zeami area (Figs 5 and 6)

The distinct nature of the NE part of the terrain surrounding Tolstoj basin was first described by Trask and Guest (1975) who referred to it as a lineated terrains unit. These terrains consist of lines of hills, scarps and valleys that extend as far as 200–300 km NE from the Tolstoy basin (Fig. 5). Trask and Guest related lineated terrains to the ejecta of an unknown basin located on the hemisphere unobserved by Mariner 10.

Schaber and McCauley (1980) interpreted this area as the radially lineated and grooved rim ejecta from Tolstoj basin. However, these authors noticed a very unusual arrangement of the ejecta: despite Tolstoj's great age and its partial embayment by the very old intercrater plains, the ejecta blanket appears to be remarkably well preserved. They also noticed that the valleys and grooves are not seen all around the basin, but only to the SW and more predominantly to the NE of the basin. They also suggested from stereophoto interpretation that the Tolstoj ejecta have been upwarped to an altitude higher than the surrounding plains.

Problems with interpreting lineated terrains as the ejecta of Tolstoj include the following points.

1. The hills and grooves are not radial to the centre of Tolstoj, but are oriented in a pattern of parallel straight lines. The grooves located in the centre of the pattern are effectively radial to the basin centre, but the grooves located near the limits of the lineated terrains show a tangential orientation to the basin.
2. Detailed stereoscopic analysis shows that the uplift of this area is an elongated bulge between Tolstoj and Zeami. The long axis of the bulge is oriented N50°. It exhibits the same azimuthal direction as the superposed grooves and hills. The NW limit of the bulge is a subdued scarp 450 km long, and corresponds approximately to the NW limit of the hills and the grooves (X–Y on Fig. 6).
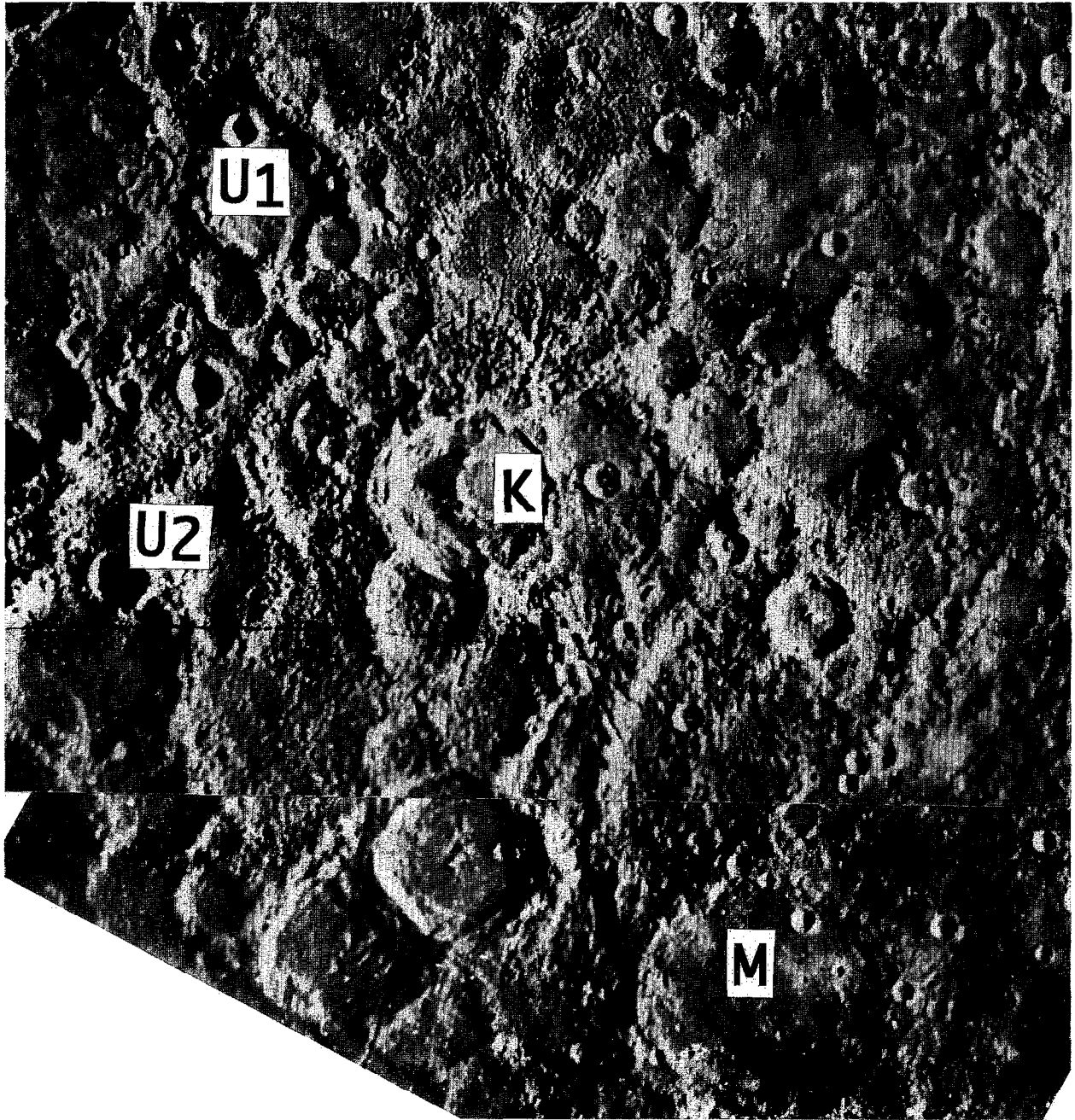
Fig. 3. Photomosaic of the Milton–Kalidasa area. Note the two troughs, U_1–U_2 and K–M. The Kalidasa–Milton trough is 250 km long. Such troughs are morphologically different from secondary crater chains which exist in the northern surroundings of Kalidasa (K)
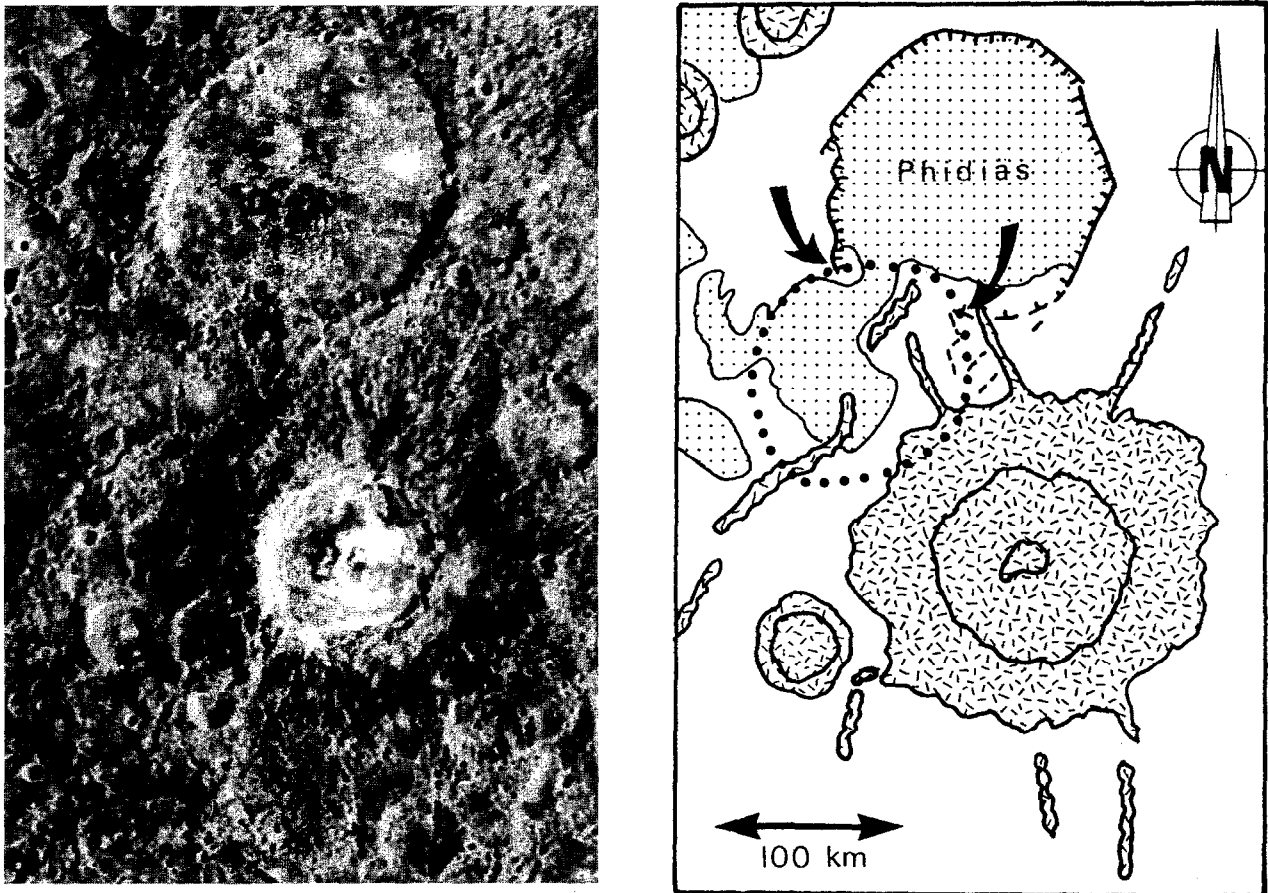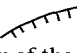
Fig. 4. Photomosaic and sketch map of the Phidias area. Shown are the intercrater plains (undashed), the smooth plains (dotted area), and the young crater material and secondaries (mottled area) around Tyagaraja crater in the centre of the picture. ⟋⟍⟍ indicates rectilinear limits of the Phidias depression, and dotted circle shows the boundary of the "ghost crater". Note that the very old ghost crater seems to transect the Phidias depression (arrows) (figure from Thomas *et al.* (1988))
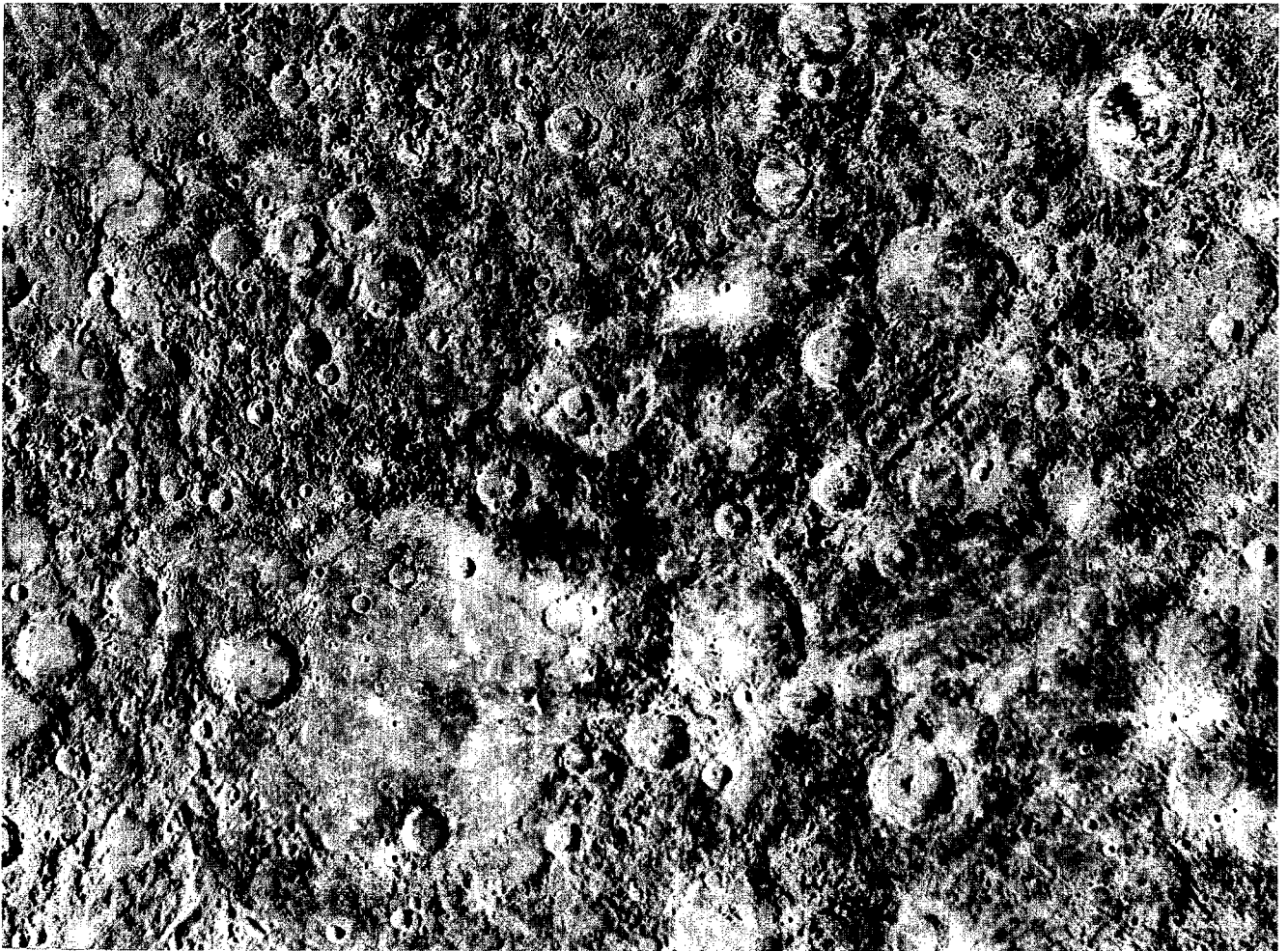
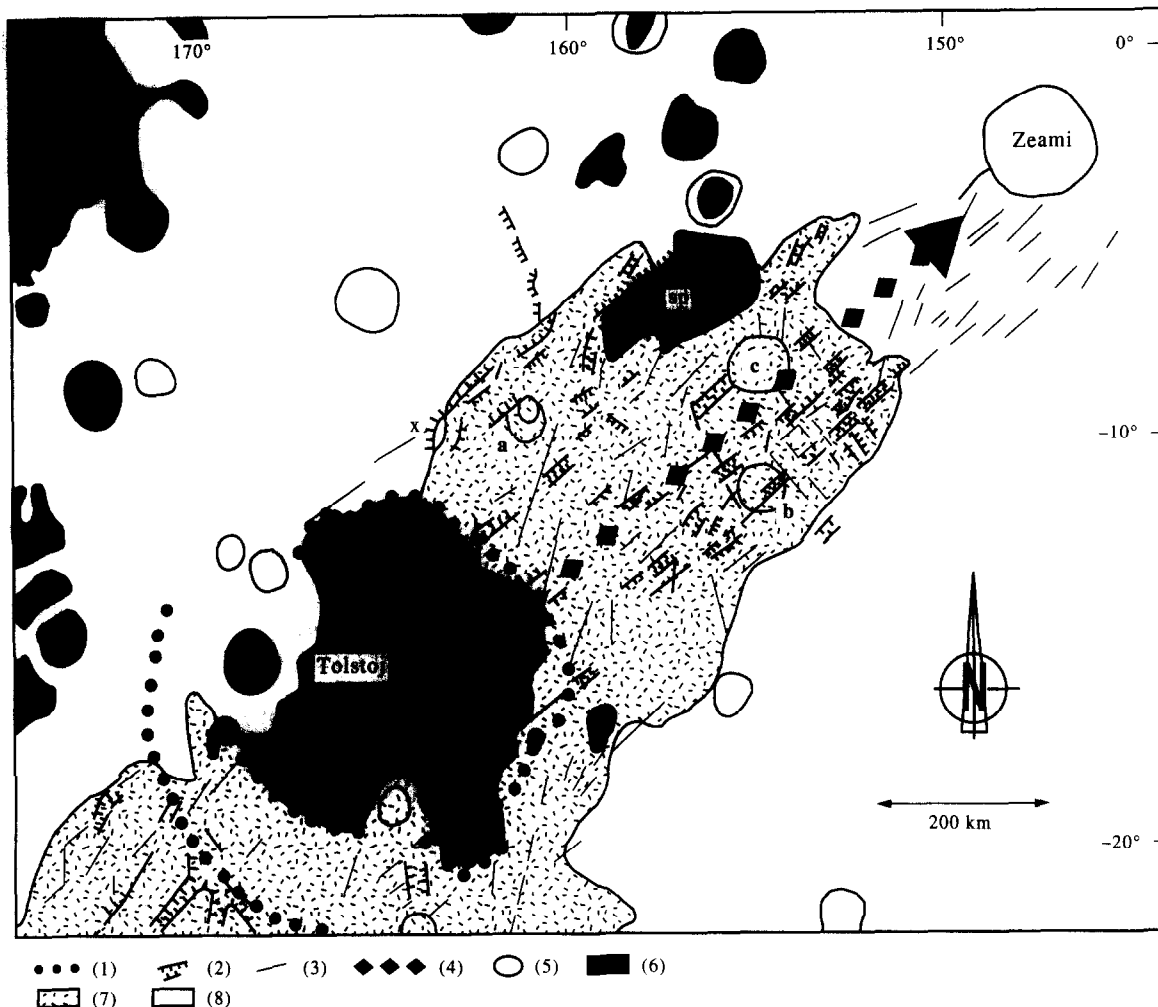**Fig. 5.** Photomosaic of the Tolstoj–Zeami area. Image is 1200 km wide

Fig. 6. Sketch map of the Tolstoj–Zeami area (figure from Thomas *et al.* (1988)). Figures 5 and 6 are represented with the same scale: (1) represent the rings of Tolstoj; (2) represent valleys and furrows; (3) represent other lineaments; (4) represent axis of the bulge; (5) represent young craters; (6) represent smooth plains; (7) represent terrains mapped as Tolstoj ejecta by Schaber and McCauley (1980); and (8) represent intercrater plains

3. The bulge and its groove and hill pattern are parallel to one of the main trends of the Mercurian grid (N50°).

4. The bulge and its grooves and hills are parallel to the long dimension of an elongated patch of smooth plains located on the flank of the bulge (SP on Fig. 6).

5. The boundary between smooth plains and intercrater plains is remarkably linear at small scale throughout the whole H8 quadrangle. The bulge is parallel to the general direction of this main boundary between the smooth plains and the intercrater plains (Fig. 7).

6. The hills and grooves affect some craters which clearly postdate Tolstoj's ejecta. The NW rim of the crater located at −10° lat., 161° long. (a on Fig. 6) is obliterated by a N50° trending ridge. This crater is classified as a C_3 crater by Schaber and McCauley (1980) and is about the same age as the smooth plains. The bottom of the C_5 crater (younger than the smooth plains) located at −11° lat., 155° long. (b on Fig. 6) is crosscut by a prominent N50° trending groove. Elsewhere (−8° lat., 155° long., c on Fig. 6), a valley seems superposed by a C_4 crater.

7. On the highest part of the bulge (near −10° lat., 153° long.), the main system of N50° trending valleys crosscuts a slightly older but clearly visible system of SE
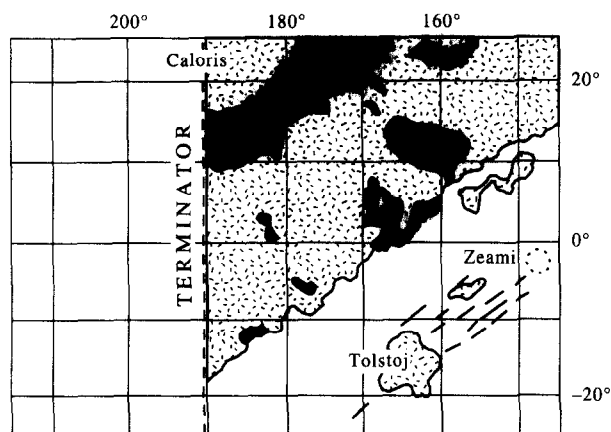

Fig. 7. Simplified geologic map of the H8 quadrangle. Shown are the Caloris ejecta (heavily shaded), the smooth plains (dotted area) and intercrater plains (unshaded area). Hatch marks indicate the Tolstoj–Zeami valleys and furrows. Note that the Tolstoj–Zeami valleys are parallel with the smooth plains/intercrater plains limit (figure from Thomas *et al.* (1988))

trending grooves that exhibit about the same morphology, but which cannot be Tolstoj ejecta.

Schaber and McCauley (1980) propose three possible

explanations for this unusual area: (1) control of the ejecta pattern by prebasin structures; (2) preferential burial along structural trends of an originally symmetrical ejecta blanket by the intercrater plains material; or (3) formation of Tolstoj by an oblique impact from the NW that produced an ejecta blanket with bilateral symmetry. None of these explanations completely accounts for the morphological and chronological characteristics of this area. Thus, we propose a tectonic hypothesis for the Tolstoj–Zeami region: the area could consist of the extensional tectonic features (horst and graben) developed on the convex top of a tectonically uplifted area. Therefore, this area would show examples of extensional features on Mercury.

Bulging is unlikely to have occurred in a single tectonic phase for the following reasons: (1) its direction is controlled by the Mercurian grid; (2) the smooth plains material limits are quite rectilinear in the NW of the bulge, and parallel to the bulge's axis. This rectilinear limit indicates that this region probably would have been soon upwarped at the time of the smooth plains flooding; and (3) some valleys are crosscut by C_4 craters, while others transect C_5 craters; the motions could have partially stopped at the C_4 times, but locally could have continued elsewhere.

Thus, it appears that the tectonic development of this area occurred over a long period of time, and is probably due to a deep and long-lived internal source, similar in some respects to Tharsis Regio on Mars, despite the large difference in the timing and scale. The existence of such large-scaled internal activity and inhomogeneities must be taken into account in further models of Mercurian internal structure and history.

These three examples show that different scale tectonic motions may occur independently of global compression or of large basin formation. Many other examples of non-understood features exist on all high resolution covered areas. Such motions could be local ones and they might be due only to "volcano-tectonic" events such as inside Phidias. But motions which affected large areas during long periods of time certainly indicate large-scale internal activity, as between Tolstoj and Zeami.

General conclusion and prospects

Mercury certainly is not a planet that has had important tectonic activity. Moreover, Mercury had three handicaps in regard to the other planetary bodies imaged during the same decade: the lowness of the image resolution, the partial coverage (which covers only 40% of Mercury) and a relatively simple geologic history, easily explained from the general point of view by global models.

Exhaustive studies of the 2500 pictures show that the despinning model only partially explains two trends of the Mercurian grid, and not the other two. Detailed morphological studies reveal that local tectonic (or volcano-tectonic) activities have occurred. Morphological and topographical studies which may be coupled together for some percentages of the surface exhibit unobstrusive vertical motions and bulging, and associated tectonic features. The long duration of such uplifting indicates

probable deep and long-lived internal sources. The available data does not allow us to further understand Mercury, and a number of puzzling questions persist. The most important problem is the complete ignorance of 60% of the surface, and the almost complete lack of quantitative topographical data. Hopefully, a future mission will answer these questions.

References

Burns, J. A. (1976) Consequences of the tidal slowing of Mercury. *Icarus* **28**, 453–458.

Dzurizin, D. (1978) The tectonic and volcanic history of Mercury as inferred from studies of scarps, ridges, troughs and other lineaments. *J. Geophys. Res.* **83**, 4883–4906.

Eppler, D. T., Erlich, R., Nummendal, D. and Schultz, P. H. (1983) Sources of shape variation in lunar impact craters. *Geol. Soc. Am. Bull.* **94**, 274.

Fielder, G. (1963) Lunar tectonics. *J. Geol. Soc. London* **119**, 65–94.

Fielder, G. (1974) Lineament pattern on the Moon, Mars and Mercury. In *Proc. Int. Conf. on New Basement Tectonic*, Vol. 1, pp. 379–387.

Fleitout, L. and Thomas, P. G. (1982) Far-field tectonics associated with a large impact basin: applications to Caloris on Mercury and imbrium on the Moon. *Earth Planet. Sci. Lett.* **58**, 104–115.

Helfenstein, P. and Parmentier, E. M. (1985) Patterns of fractures and tidal stresses due to non synchronous rotation: implications for fracturing on Europa. *Icarus* **61**, 175–185.

McKinnon, W. B. (1981) Application of ring tectonic theory to Mercury and other solar system bodies. In *Multi-ring Basins*, *Proc. Lunar Planet. Sci.*, eds P. H. Schultz and R. B. Merril, Vol. 12(A), pp. 259–273.

Masson, P. and Thomas, P. G. (1977) Preliminary results of structural lineament pattern analysis of Mercury. Rept Planet. Geol. Prog., NASA TM 3511, pp. 54–55.

Melosh, H. J. (1977) Global tectonics of a despun planet. *Icarus* **31**, 221–243.

Melosh, H. J. (1980a) Tectonic pattern on a tidally distorted planet. *Icarus* **43**, 334–337.

Melosh, H. J. (1980b) Tectonic pattern of a reoriented planet: Mars. *Icarus* **44**, 455–745.

Murray, B. C. and the Mariner 10 Imaging Team (1974) Mercury's surface, preliminary description and interpretation from Mariner 10 pictures. *Science* **185**, 169–179.

Murray, B. C., Strom, R. G., Trask, N. J. and Gault, D. E. (1975) Surface history of Mercury: implications for terrestrial planets. *J. Geophys. Res.* **80**, 2508–2514.

O'Donnell, W. P. (1980) The surface history of the planet Mercury, Ph.D. Thesis, University of London.

Pechmann, J. B. and Melosh, H. J. (1979) Global fracture patterns of a despun planet: application to Mercury. *Icarus* **38**, 243–250.

Schaber, G. G. and McCauley, J. F. (1980) Geologic map of the Tolstoj quadrangle of Mercury (H8), U.S. Geol. Surv. Map I-1199.

Schultz, P. H. and Gault, D. E. (1975) Seismic effects from major basin formation on the Moon and Mercury. *The Moon* **12**, 159–177.

Spudis, P. D. and Guest, J. E. (1988) Stratigraphy and geologic history of Mercury. In *Mercury*, eds F. Vilas, C. Chapman and M. Matthews, pp. 118–164. University of Arizona Press, Tucson.

Strom, R. G. (1964) Analysis of lunar lineaments I: tectonic maps of the Moon. *Commun. Lunar Planet. Lab.* **2**, 205–216.

Strom, R. G., Trask, N. J. and Guest, J. E. (1975) Tectonism and volcanism on Mercury. *J. Geophys. Res.* **80,** 2478–2507.

Thomas, P. G. (1978) Structural lineament pattern analysis of the Caloris surroundings: a pre-Caloris pattern on Mercury, Rept Planet. Geol. Prog., NASA TMX 79-929, pp. 79–82.

Thomas, P. G. and Masson, P. (1983) Tectonic evolution of Mercury: comparison with the Moon. *Ann. Geophys.* **1,** 53–58.

Thomas, P. G. and Masson, P. (1984) Tectonic of the Caloris area on Mercury: an alternative view. *Icarus* **58,** 396–402.

Thomas, P. G., Masson, P. and Fleitout, L. (1988) Tectonic history of Mercury. In *Mercury*, eds F. Vilas, C. Chapman and M. Matthews, pp. 401–428. University of Arizona Press, Tucson.

Trask, N. J. and Guest, J. E. (1975) Preliminary geologic terrain map of Mercury. *J. Geophys. Res.* **80,** 2462–2477.